3.7 The RF System for the Main Linacs

The basic design of the NLC main linacs rests on global experience gained from the design, construction, and 30 years of operation of the 3-km-long SLAC linac, which is powered at a frequency of 2.856 GHz [2, 3]. Since its initial operation in 1966, the SLAC linac has been continuously upgraded for higher energy, higher intensity, and lower emittance.

The radio frequency (rf) system for the NLC main linacs is similar in character to the SLAC linac. The SLAC linac is currently energized by 240 high-power S-band klystrons. The klystron peak power and pulse duration are, respectively, 65 MW and 3.5 μs. The power from each klystron is compressed by a SLED pulse compressor, and then split to feed four, 3-m-long, constant-gradient, S-band accelerator structures operating in the $2\pi/3$ mode.

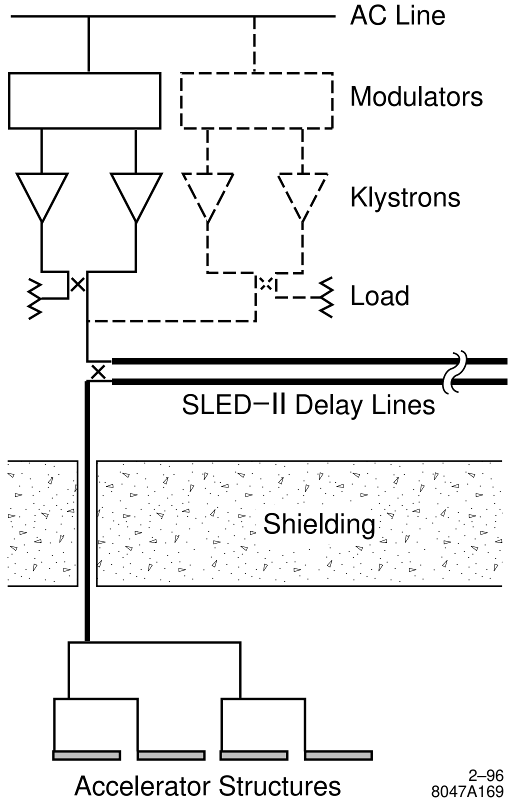

Figure 3.16: Schematic of one module of the high-power rf system for the main linacs. Dashes indicate additions for the beam-energy upgrade from 250 GeV to 500 GeV.

When the SLAC linac was built, the accelerating gradient was 7 MV/m. The original design included a future upgrade path in which the number of klystrons would be quadrupled. The upgrades that were eventually implemented involved replacing each of the initial 24-MW klystrons with a single higher-power klystron (first with 35-MW, XK-5 tubes and, later on, with 65-MW, 5045 tubes), and adding a SLED pulse compressor downstream of each klystron. For present-day SLC operations, fully upgraded with 240 SLEDed, 65-MW klystrons, the accelerating gradient has been tripled, to 21 MV/m, and the maximum beam energy is 60 GeV (for unloaded, on-crest operation).

The rf power system for the NLC's two high-gradient linacs that accelerate the electron and positron beams separately from 10 GeV to 250 GeV in the initial design, and to 500 GeV or more after the upgrade, operates at 11.424 GHz. This system includes all the hardware through which energy flows, from the AC line to the accelerator structures. Figure 3.16 shows one module of the rf system schematically.

Electrical energy is transformed at each stage shown in the diagram: the modulator converts AC power into high-voltage pulsed DC, the klystron transforms pulsed DC into high peak power rf, the SLED-II pulse-compression system increases the peak power by about a factor of four (at the expense of a reduced pulse width), and the accelerator sections convert rf power into beam power. Because of the high average rf power required to drive the accelerator structures, it is important that the highest possible efficiency be maintained for the processing and transmission of energy at every stage of the rf system.

The primary technical choice for the rf system is the use of the 11.424-GHz frequency. This frequency, high in the X-band (8.2–12.4 GHz), is exactly four times the operating frequency of the existing SLAC 60-GeV linac. The choice of such a high frequency, relative to existing high-energy linacs, allows higher accelerating gradient, shorter linac length, and lower AC power consumption for a given beam energy. Considering the size, weight, cost, and availability of standard microwave components, we have chosen a frequency in the X-band for a design that is upgradable from an initial 250-GeV beam energy to 500 GeV or more.

The general parameters of the high-power rf system and its major subsystems (klystrons, modulators, rf pulse compressors, and the accelerator structure itself) are specified in Table 3.10. The set of parameters has been optimized to provide high acceleration gradient (35–64 MV/m) for trains of bunches with a moderate charge per bunch (1.2–1.8 nC). This optimization keeps single-bunch wakefields under control and reduces the beamstrahlung at the collision point to tolerable levels. The upgrade to 500-GeV beam energy (1-TeV center-of-mass energy) is accomplished by doubling the number of modulators (as shown by dashed lines in Fig. 3.16), and by replacing each 50-MW klystron with a pair of 75-MW klystrons. The total active length of linac must also be increased from 16,300 m to 17,700 m. The upgrade plan also includes improvements in the modulator and pulse compression systems to increase the rf system efficiency.

The design of the high-power X-band rf system for the NLC is based on specific experience gained from building X-band prototypes and operating them at high power, and on an rf systems-integration test—the Next Linear Collider Test Accelerator (NLCTA)—which is currently under construction at SLAC. The goals of the NLCTA project [4, 5] are to integrate the technologies of X-band accelerator structures and high-power rf systems, to demonstrate multibunch beam-loading energy compensation and suppression of higher-order beam-deflecting modes, to measure any transverse components of the accelerating field, and

Table 3.10: NLC main linac rf system parameters.

	NLCTA Achieved	500-GeV Design Goal	1-TeV Upgrade
General Parameters			
Frequency (GHz)	11.4	11.4	11.4
Accel. Gradient (MV/m), Unloaded/Loaded	67/–	50/35.3	85/63.5
Overhead Factor,[1] F_{OH}		1.20	1.15
Active Linac Length[2] (m)		16,300	17,700
Total Linac Length = 1.08 × Active Length (m)		17,600	19,100
Number of Modulators		2264	4908
Number of Klystrons		4528	9816
Peak Power per meter of Structure (MW/m)		50	145
Rf Pulse Length at Structure (ns)	150	240	240
Repetition Rate (Hz)	60	180	120
Particles per Bunch (10^{10})		0.75	1.10
Number of Bunches per Pulse		90	90
Peak Beam Current (A)		0.86	1.26
Total Average RF Power at Structure [3] (MW)		34.1	71.3
Klystron			
Output Power (MW)	50, 75	50	75
Pulse Length (μs)	2.0, 1.1	1.2	0.96
Microperveance ($\mu A/V^{3/2}$)	1.2	0.6	0.75
Electronic Efficiency[4] (%)	48	57	60
Beam Voltage (kV)	440	465	487
Focusing	Electromagnet	PPM	PPM
Cathode Loading (A/cm^2)	7.4	7.4	7.6
Modulator (Blumlein PFN, transformer ratio 7:1)			
PFN Voltage (kV)	48	68	71
Pulse Rise Time (ns)	400	275	175
Net Modulator Efficiency (%)	58	72	75
RF Pulse Compression			
System Type	SLED-II	SLED-II	BPC/DLDS
Compression Ratio	5–7	5	4
Intrinsic Efficiency (%)	80–69	80	100
Pulse Compression Efficiency (%)	73–64	76.5	93
Power Transmission Efficiency (%)	90	94	94
Net Pulse-Compression Efficiency (%), Including Power Transmission Loss	66–58	72	87.5
Net Power Gain	3.3–4.1	3.6	3.5
Net RF System Parameters			
Total AC Power (MW), Excl. Aux.		116	181
Rf System Efficiency (%), Excl. Aux.	19	29.6	39.4
Total Auxiliary Power[5] (MW)		5.4	12
Total AC Power (MW), Incl. Aux.		121	193
Rf System Efficiency (%), Incl. Aux.		28.2	37.0
Average Beam Power (MW), Excl. Injected		9.3	18.6
AC-to-Beam Efficiency (%)		7.7	9.4

[1] Includes overhead for BNS damping, feedback, and stations off for repair.
[2] Active length = F_{OH} (E_0 − 20 GeV)/(Loaded Gradient).
[3] Assumes 3% of klystrons and modulators are off (repair margin) or running off beam time (on standby).
[4] Given by simulated efficiency less 5 percentage points for 500-GeV design; equal to simulated efficiency for 1-TeV design.
[5] Includes klystron cathode heater power, thyratron heater and reservoir power, and power for modulators on standby (0.5%).

to measure the growth of the dark current generated by rf field emission in the accelerator.

The NLCTA's 160-kV electron gun has been commissioned. The 70-MeV, X-band injector module and two of the three 130-MeV, X-band linac modules of the NLCTA are expected to become operational in 1996, with each module powered by a single 50-MW klystron. The first accelerator physics experiments are planned for 1996–1997. The last linac rf module (including the fifth and sixth 1.8-m-long X-band sections) is planned to be installed in 1997. It is expected that an upgrade from 50-MW klystrons to 75-MW klystrons will occur gradually as the new higher-power tubes become available through the klystron development program.

3.7.1 Klystrons

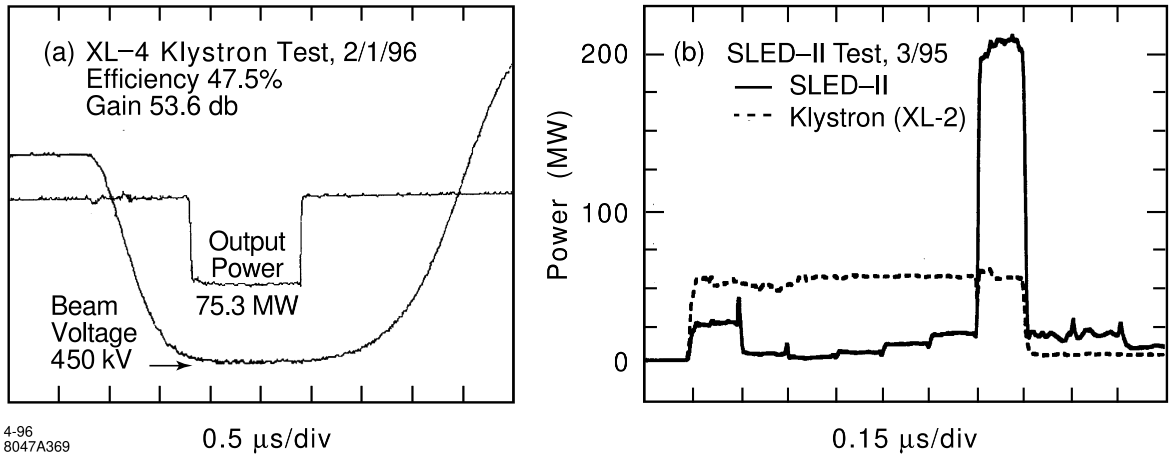

Figure 3.17: High-power tests of (a) an X-band klystron and (b) a SLED-II pulse compressor.

Obtaining the X-band peak power for the NLC has required the development of klystrons capable of delivering peak power significantly greater than previously achieved by commercially available X-band sources. Both the peak power and the pulse length required for the NLC design and upgrade have already been achieved by solenoid-focused X-band klystrons at SLAC. Four prototypes now produce 50-MW pulses, over 1.5 microseconds long, with performance characteristics that are correctly modeled by computer codes. The most recent prototype produces 75-MW pulses, one microsecond long, and exhibits electronic efficiency of 48% (Fig. 3.17). These klystrons will be used to power the NLC Test Accelerator.

The solenoid which focuses the electron beam in the prototype klystrons has a weight of 750 kg and a power consumption of 20 kW. Currently nearing completion is the first prototype of a 50-MW klystron which is focused instead by a periodic permanent magnet (PPM) array of samarium-cobalt ring magnets weighing about 9 kg. It is this klystron, which operates at a higher voltage and lower beam current for compatibility with PPM focusing, which is slated as the prototype for the NLC. Based on computer projections, the tube, designated X5011, is expected to operate at about 57% efficiency with 50 MW of peak output power. This first, high-power PPM klystron, which is shown in Fig. 3.18, was fabricated and tested as a beam tester (a klystron without rf cavities) to validate the beam focusing. Beam transmission in excess of 99.9% was achieved without the magnet trimming which is customarily required for traveling-wave tubes which are PPM focused. The klystron prototype with rf cavities has been fabricated and is being readied for beam and rf tests.

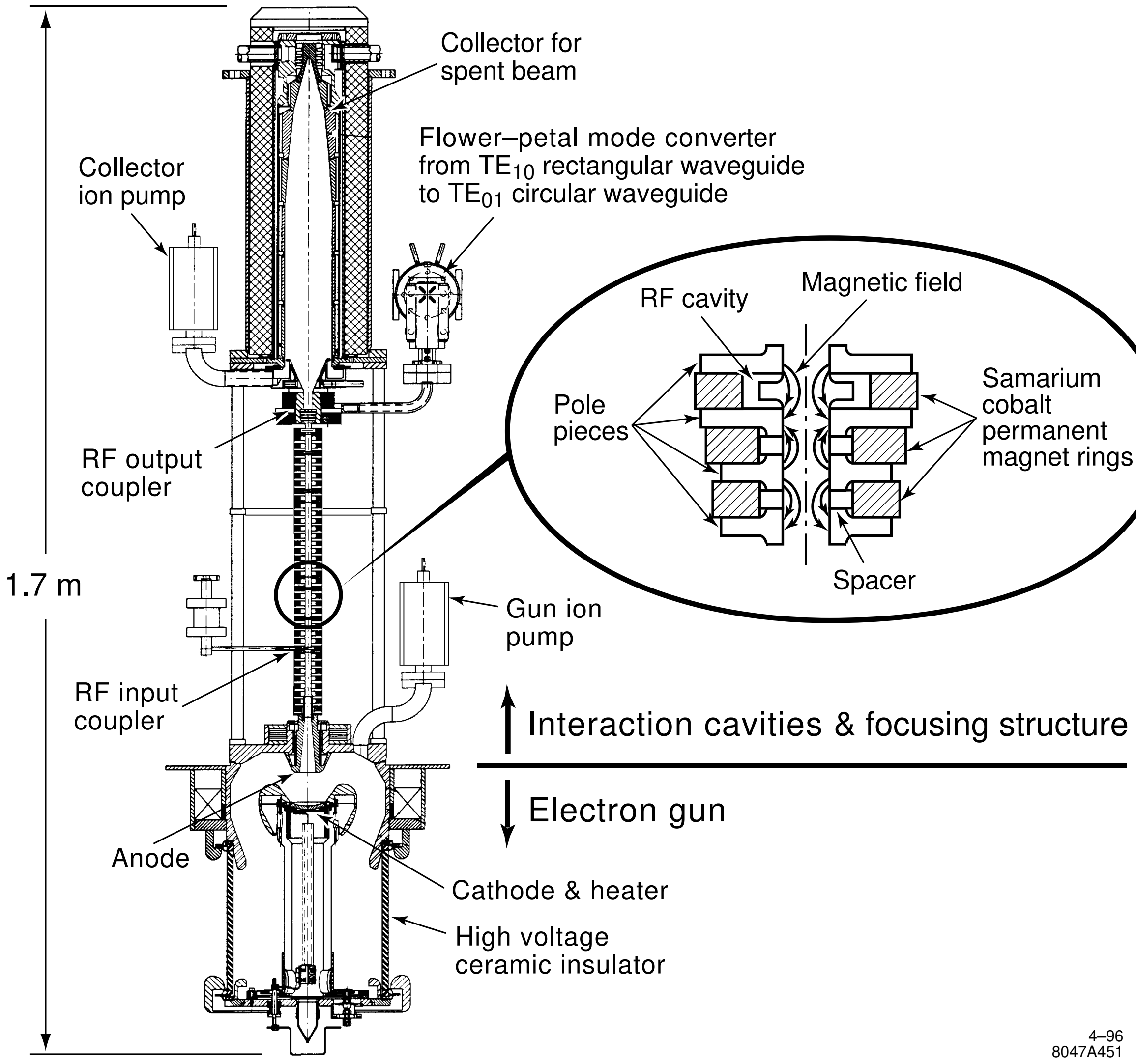

Figure 3.18: Preliminary layout of the X5011 PPM klystron, with water jacket removed. The insert shows one representative buncher cavity, to illustrate the use of oversize permanent magnets.

3.7.2 Modulators

Each high-power rf station consists of a pair of PPM-focused klystrons (50 or 75 MW) and a pulsed-DC energy delivery system (modulator) that is tightly integrated in design with the electron guns of the klystrons. The pulsed-DC energy delivery system includes a single-thyratron switch, a Blumlein pulse-forming network (PFN), a high-efficiency power supply for charging the PFN's capacitance, and a pulse transformer. Using a Blumlein PFN allows for a relatively low transformer turns ratio (7:1), which yields a reasonably fast rise time (0.3 μs), and hence, an improved efficiency.

The technology for standard line-type high power pulse modulators is very mature. The SLAC linac has been in operation for about 30 years using about 240 such modulators to drive the high-power klystrons. The efficiency of these modulators for converting wall-plug power into klystron beam power in the flat-top portion of the high voltage output pulse is about 60%. Similar modulators have been constructed for the NLC Test Accelerator, and are currently under test. Parameter values for these modulators are listed under the "NLCTA Achieved" column in Table 3.10. The net efficiency for the NLCTA modulator is 58%.

A key consideration for a modulator in a linear collider application is efficiency. A 1% relative decrease in modulator efficiency would result in an increase by between one and two megawatts in the AC line power required for the NLC rf system. It is clear that efficiencies for the SLC and NLCTA modulators are too low for consideration for the NLC.

An important component in determining the modulator efficiency is the pulse transformer. The pulse forming network (PFN) delivers a more-or-less rectangular pulse to the primary of the pulse transformer when the thyratron switch is triggered. The voltage pulse delivered to the klystron, however, contains a considerable amount of wasted energy in the rise and fall-time portions of transformer output pulse. In practical pulse transformer designs, it is observed that the rise time (and fall time) is determined in large measure by the transformer turns ratio: a high turns ratio implies a longer rise time, and vice versa. For the NLCTA modulator, a pulse transformer with a turns ratio of 21:1 is required to step up a 48-kV PFN voltage to the 500 kV required by the NLC klystron. This ratio can be reduced to about 14:1 by increasing the PFN charging voltage from 48 to 72 kV. This, of course, requires a thyratron with a higher voltage hold-off capability. A further reduction in transformer ratio to 7:1 can be achieved by using a voltage-doubling, or Blumlein, PFN configuration. Simulations show that a pulse-shape efficiency of about 80% can be achieved for this turns ratio. Combining this with an estimated efficiency of 93% for the DC power supply which charges the PFN, and assuming an additional 3% is lost in the voltage drop across the thyratron and other series resistances, the net efficiency for such a modulator design is estimated to be about 72%.

The R&D task for the NLC modulator group is to show that such an efficiency can be obtained in practice in a prototype modulator. Several possibilities are under consideration for the Blumlein PFN using both lumped capacitors and smooth transmission lines. Appropriate R&D is underway to design and construct prototype PFN configurations. Techniques for improving pulse transformer efficiency are also under investigation.

3.7.3 RF Pulse Compression and Power Transmission

The 1.2-μs-long X-band klystron pulses will be compressed by a factor of five—to 0.24μs—using the SLED-II rf pulse compression technique [6]. SLED-II is a modification of the SLED [7] compressor is used to increase the rf power into the 60-GeV SLAC linac by a factor of about 3.

A SLED-II pulse compressor works by storing microwave energy in a pair of high-Q resonant delay lines for most of the duration of the klystron pulse. The round-trip transit time of the rf in the delay lines determines the duration of the compressed pulse. Developmental SLED-II systems have been tested at SLAC with high-power X-band klystrons to validate the design and its components [8, 9, 10]. The peak power and efficiency needed for the NLC Test Accelerator have been demonstrated in a prototype system (Fig. 3.17). Three SLED-II systems are being manufactured for the NLCTA. Further validation of the SLED-II design at the higher power levels and efficiencies needed for the NLC will be performed in upgrades to the NLCTA. The rf pulse compression systems in the NLC and NLCTA are designed to accommodate future upgrades in which the peak rf power is nearly tripled, by replacing each 50-MW klystron with a pair of 75-MW klystrons.

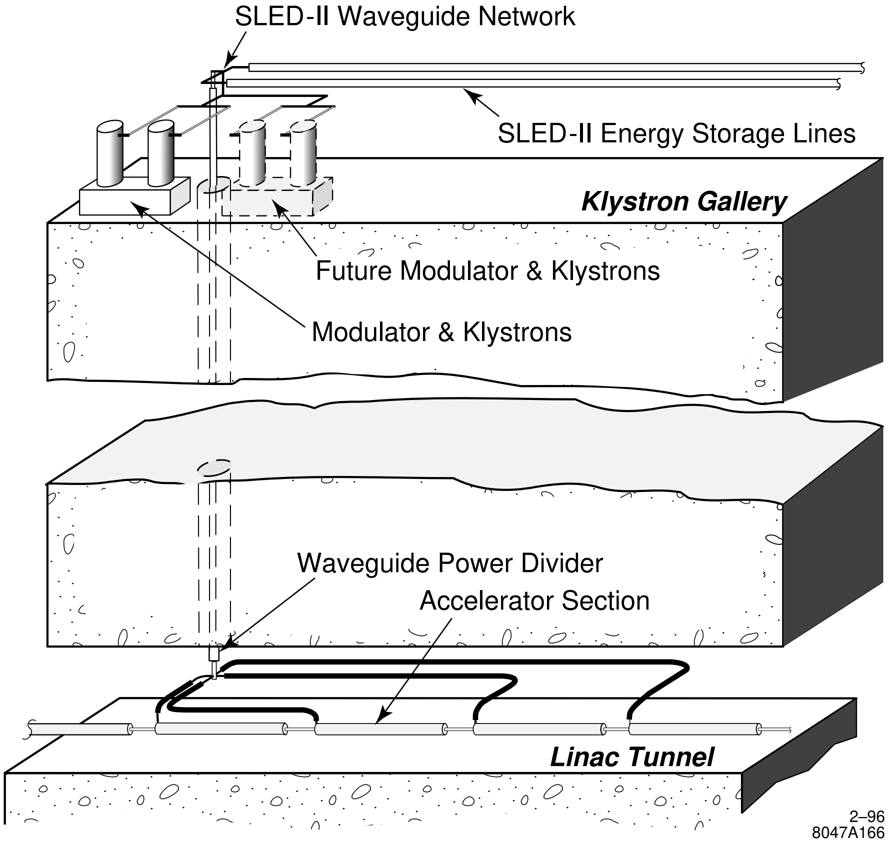

Figure 3.19: Physical layout of the waveguide network for rf pulse compression and power transmission.

Figure 3.19 illustrates the physical layout of the waveguide network for rf pulse compression and power transmission to four 1.8-m-long linac sections in a two-tunnel (SLAC-type) configuration. The waveguide layout is sufficiently flexible to absorb the absolute motion of the accelerator sections due to their mechanical movers ($\pm$ 1 mm) and the relative motion between the klystron gallery and the accelerator tunnel due to settling ($\pm$ 10 mm). The SLED-II waveguide networks are located in the low-radiation environment of the klystron gallery so that the rf pulse-compression system may be modified, station by station, if necessary for upgrade to higher beam energies, simultaneously with colliding beam operations.

Since the round-trip delay time in the 4.75-in-diameter waveguide (at the group velocity, $0.964c$) must equal the rf pulse duration (0.24 μs), the physical length of the SLED-II delay lines is 35 m. The physical layout can accommodate this delay-line length by spatially overlapping the delay lines from adjacent rf stations. Since the total length of linac fed by each rf station is approximately eight meters, each pair of delay lines will overlap parts of five other pairs of delay lines.

3.7.4 Accelerator Structure

The design of the X-band accelerator structures for the NLC is based on theoretical and experimental experience gained by modeling and building accelerator structures for the NLCTA and operating them at high gradients.

One of the main challenges is to suppress the deflecting modes that will otherwise cause severe multibunch emittance growth in the NLC linacs. Suppression of the transverse wakefield will be achieved through a combination of precision alignment and by detuning and damping higher-order modes. Another challenge in the design of the accelerator structures for the NLC is suppressing field emission at the high-surface field gradients encountered in these structures. This suppression, so far, has been achieved through machining, processing, and handling techniques that minimize surface roughness and eliminate contamination of the high-gradient surfaces. Other, additional methods may be adopted later.

The rf accelerator structure is designed to be very nearly a constant-gradient traveling-wave structure. The design of the structure has been optimized to suppress the wakefield seen by trailing bunches. This has been accomplished by tailoring the cell-to-cell frequency distribution of the dominant deflecting mode to yield an initial Gaussian-like decay of the wakefield amplitude. On a longer time scale, the higher-order beam-induced modes of the structure will be damped by vacuum manifolds to which each cell of the structure is coupled. This structure is designated by the acronym DDS (damped detuned structure). The damping manifolds run parallel to the beam channel and are terminated into matched loads. (The slots that couple the cells to the manifolds are cut off to the fundamental accelerating mode.) This damping scheme will reduce the typical quality (Q) factors of the deflecting modes to about 1000. The first prototype 1.8-m-long X-band accelerator section, which was detuned but not damped, was high-power tested up to a gradient of 67 MV/m. The effect of the detuning in that first prototype section was demonstrated experimentally by using positron and electron bunches from the SLC damping rings as probe and witness beams, respectively. Another prototype 1.8-m section that is both damped and detuned is being manufactured and will be used for a similar test before it is installed in the NLCTA.

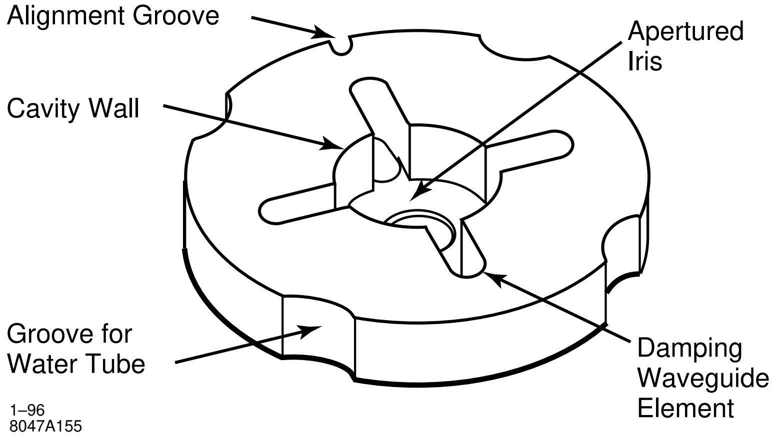

Figure 3.20: Basic cell design.

The basic features of the cell are shown in Fig. 3.20. The central portion is the conventional "cup" consisting of a cylindrical cavity wall and an apertured iris which, when stacked in a row with other cells, forms the disk-loaded waveguide accelerator structure. The diameter of the cavity wall, the thickness of the iris, and the diameter of its aperture vary progressively from cell to cell to "detune" the beam-deflecting dipole modes and suppress cumulative build-up of wakefields, while maintaining the quasi-constant-gradient characteristics of the fundamental accelerating mode. The central cavity is slot-coupled to four outer rectangular holes. When the cells are stacked, the holes form four waveguides which run parallel to the axis of the structure. When terminated in matched loads, the four waveguides become "damping manifolds." The slots (which are cut off for the fundamental accelerating mode) couple power from beam-excited dipole modes into these damping manifolds, lowering the Q and suppressing long-range wakefield build-up. Microwave signals from the damping manifolds can be used to monitor the alignment of the structure with respect to the beam.

For a single detuned accelerator section, the fractional spacing for the fundamental dipole-mode frequencies (near the center of the gaussian distribution of frequencies) is about 3×10^{-4}. Machining precisions for conventional machining and diamond-point machining (obtained at KEK), and alignment tolerances of stacks of cells, are given in Table 3.11. Since the cell radius is about a centimeter, diamond-point machining should produce a random frequency error, for the fundamental dipole modes, somewhat less than the spacing between the frequencies. The systematic error should be significantly less than this.

Misalignment tolerances, on scales ranging from a few cells within a structure to several structures, were discussed in the preceding section. It was found that the tightest tolerances occurred for the alignment of groups of about 20–40 cells. Thus, great care must be taken in brazing together the subsections of complete structures after their initial assembly from individual cups.

The goal is an accelerator section 205 cells long (plus the input coupler) in which the axes of the individual cavities lie on a straight line to within 15 μm (rms). To avoid a cumulative tolerance build-up which exceeds this goal, many other cell dimensions have to be held to tolerances in the 2 to 3 μm range. This applies particularly to the diameter and coaxiality of the outer surface of the cell, since this has to be the reference surface used in stacking the cells prior to bonding. It also applies to the perpendicularity, flatness and parallelism of the cell faces. Errors here will cause "bookshelving" of the cells in the cell stack [11]. Equally important is the coaxiality of the iris aperture with respect to the cavity outer wall. These tight tolerances on cavity dimensions (including the thickness of the iris and the radius of its edge) are also necessary to achieve the design fundamental and dipole-mode frequency characteristics, because provision for tuning after assembly has been eliminated. Flatness of cell faces is also essential to achieve diffusion bonding (discussed below) over relatively large surface areas with a very low expected failure rate.

Table 3.11: Cell machining and assembly tolerances achieved (in microns).

	Detuned 1.8-m Section #1	Detuned 0.9-m Sections #1&2	Detuned 1.8-m Section #2 and DDS #1
Machining Technique	Conventional	Conventional	Diamond-point
Alignment Technique	Nesting	Vee-Block	Vee-Block
Diameters	±7	±7	±2
Concentricity	10	10	1
Thickness	±7	±7	±2
Parallelism	10	10	0.5
Flatness	10	10	0.5
Surface Finish	0.4	0.4	0.05
Cell-to-cell Alignment of Outer Cylindrical Surfaces:			
(a) Expected	22	10	3
(b) Measured after diffusion bonding or brazing	10	6	4

Single-crystal diamond-point machining is to be used on all surfaces of each cavity, the cell faces and outer periphery. The hardness, high thermal conductivity, and low thermal expansion of diamond result in a superior tool which, when used in a vibration-free lathe, yield mirror-like surfaces on copper which have a roughness of 0.1 μm or less. This finish is necessary to obtain good diffusion bonding, high Q factors, low dark current and high power-handling capability. The sharpness, mechanical stability, and minimal wear of the tool allow the dimensional tolerances to be met.

Table 3.11 illustrates what tolerances on dimensions and alignment have been achieved to date at SLAC, and what can reasonably be expected with the best technology available today. It can be seen that the most significant advances have been made by resorting to diamond-point machining and by using precision granite vee-blocks to align the stacks of cells prior to brazing or diffusion bonding. Cells designed to nest into each other have to fit loosely enough to permit assembly without galling, and this can result in unacceptable misalignment. Our present experience is that stacks of 38 cells can have a bow of a few tens of microns after diffusion bonding. This can be reduced to a few microns by setting the stack horizontally in cradles on a granite block and applying bending forces while monitoring movement with a precision coordinate measuring machine.

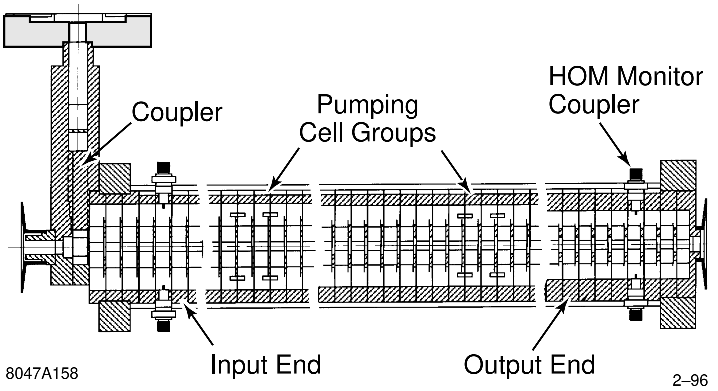

Figure 3.21: Longitudinal cross section of a 1.8-m long X-band accelerator section.

In addition to direct pumping along the beam-interaction region, the structure is pumped in parallel by the four damping waveguides. Two groups of four special pumping cells will be inserted into the structure, at points one-fourth of the section length from each end. A longitudinal cross section of the accelerator section is shown in Fig. 3.21. Each pumping cell group is connected to two pumps via short transverse manifolds.

Figure 3.21 shows no output coupler. The intention is to provide internal matched terminations for both the fundamental accelerating mode and the wakefield modes by depositing lossy coatings on the walls of the cavities and the damping manifolds in the last four cells. A coaxial loop loosely coupled to the last cavity will be used to monitor the fundamental-mode power. This signal will pass through a coaxial rf window in the cell wall, and will be used by the klystron phasing system. However, if satisfactory internal terminations cannot be developed, external loads and couplers will have to be used.

Mass Production of Accelerator Cells

The two main linacs will contain about 1.8 million cells, which have to be produced in about three years. Assuming that a specialized plant set up to fabricate the cells operates 50 weeks per year at two shifts per day, then, at 80% efficiency, a production rate of about two cells per minute is required. A close estimate of the time taken to machine a single cell cannot be made without reference to specific machines and machining techniques. (See, for example, the study reports prepared for the CERN CLIC cells [12, 13].) However, very rough estimates may be drawn from those reports, noting that the surface area of the X-band DDS cell is about three times that of the CLIC cell. All the features of the DDS cell shown in Fig. 3.20 could be machined to conventional tolerances on the end of bar stock (leaving excess material on the critical surfaces to be diamond-point machined in subsequent operations), using a multipurpose CNC turning and milling machine. The cell could thus be cut from the bar using a parting-off tool, stress-relieved and delivered to a diamond-point lathe for finishing in two steps. In the first step, the cell could be gripped on the outside by a precision chuck while the back face is diamond turned. In the second step, the back face could be held in a vacuum chuck while the front face and cavity surfaces are diamond finished. Based on estimated operation times, the plant will need a minimum of 22 conventional CNC turning and milling machines and 8 diamond-point lathes, with appropriate numbers of all supporting equipment (automatic handling and transfer machines, stress-relieving ovens, cleaning, QC, and packing stations) to maintain the required throughput.

High-power Tests and Dark Current Studies

The theoretical and experimental studies on the behavior of copper accelerator structures under extremely high-rf fields have been carried out at SLAC for several years [14, 15]. We have studied in considerable detail the problems of rf breakdown and dark current generated by field emission at high gradient. The dark current may absorb rf energy, get captured, and produce undesirable steering effects and detrimental X-ray radiation. Many experiments have been done to measure the amplitude and energy spectrum of the dark current and to study phenomena related to rf breakdown such as outgassing, radiation, heating, etc. We have concluded that the dark current can be minimized by improving surface finish and cleanliness, and by rf processing.

High-power tests with an electron beam have demonstrated that the 1.8-m section is properly tuned to 11.424 GHz and can accelerate a beam at a gradient of more than 67 MV/m. Dark current from this structure was measured in a Faraday cup as a function of average accelerating field (Fig. 1.8), and found to be negligible for an accelerating gradient of 50 MV/m was found to be negligible. At 85 MV/m. The energy spectrum of the dark current was measured and found to be sufficiently low that the quadrupoles will overfocus and sweep the field-emission current away from the primary, high-energy beam.

Experiments performed with S-band accelerators at KEK [16, 17] have shown that the dark current produced by field emission from the accelerator disks is reduced by an order of magnitude when stringent precautions are taken to exclude dust during fabrication, assembly, processing and testing. These experiments indicate that the NLC accelerator cells should be cleaned in ultra-pure, dust-free chemical solutions and rinses, assembled and bonded under clean-room conditions, and perhaps given a final rinse in ultra-pure water before vacuum bakeout and installation. We expect application of these procedures to our X-band structures to yield equally significant improvements.

3.7.5 RF Drive and Phasing Systems

To achieve a highly monoenergetic multibunch beam pulse for the final focus, the beam loading induced by the bunch train must be compensated. The initial transient can be eliminated by pre-loading the sections by shaping the input rf pulse using an approximately linear rise of the field amplitude for one filling time of the structure. In this way, the first electron bunch will see a filled rf structure that appears to be in the steady state. This requires phase-agile control of the rf before it is amplified by the klystron.

The design of the rf drive and phasing systems for the NLC will be based heavily on experience gained from existing systems developed for the SLAC linac and its 60-GeV upgrade for the SLC, with further extensions based on the design of the NLCTA. The challenges to be met for the NLC arise from its greater length, number of components that must be controlled, required tolerances, maintainability, and reliability. The requirements imposed on the rf drive and phasing systems are summarized below:

- The drive system must provide stable, adjustable, and reliable input power to 4528 klystrons (approximately 1-kW pulsed peak power per tube). The layout of the system must be such that individual subsystem failures do not cause the beam energy to decrease to less than 85% of its operating level. This requirement is dictated by potential collimator and other damage caused by off-energy beams.

- The amplitude of the drive power must be adjustable so as to individually saturate the high-power klystrons.

- The phase of the drive power must be adjustable in several ways:

  - Slowly, to take care of phase drifts and drifts caused by length changes in equipment and terrain. Included here are the couplers, coax lines, intermediate amplifiers, high-power klystrons, SLED-II, waveguide components, and the changes in time at which the bunch trains are injected into the X-band linacs by the S-band bunch compressors.
  - Quickly (within each 1.2-μs klystron rf pulse), to create the proper resultant amplitude and phase profiles necessary to produce the desired fields in the accelerator structures and to place the bunches at the desired phase positions with respect to the X-band waves. These positions are dependent on bunch number and charge,

which can change from pulse to pulse, and are dictated by BNS phasing, single bunch and multibunch beam loading, and other considerations.

– The phasing system design must also include initial adjustments (upon installation) of the waveguide runs which feed the four accelerator sections driven by one pair of klystrons in a station.

The phases of the high-power rf fields which act on bunch trains should be adjusted with an accuracy of about $0.5°$ at 11.424 GHz. A schematic layout of the rf drive and phasing system for the NLC is shown in Fig. 3.22.

There are various schemes for providing the approximately 1 kW of pulsed rf needed to drive each high-power klystron. It is useful to have individual drivers because the various phase manipulations involved in the operation of the rf compressors are best done at the milliwatt level. Power-combining of the two klystrons on the single modulator is done by phase modulation of the two klystron inputs by equal amounts in opposite directions. This has the effect of sending the desired vectorial sum into the rf pulse compressor and dumping the vectorial difference into a load.

There exists extensive Traveling Wave Tube (TWT) technology at this frequency and power level as a product of military applications. The available TWTs are reliable, but fairly complex to manufacture and operate. They have already been extensively cost-optimized, and are still very expensive.

Alternatively, a small X-band driver klystron of fairly narrow bandwidth and modest gain could be designed. In construction, it would be relatively simple compared to a TWT. It is possible that after the initial engineering models are tested, a modest program of redesign for automatic manufacturing could significantly reduce the unit cost.

3.7.6 Upgrade to 1 TeV

An essential goal of the NLC is that it be possible to increase the center-of-mass energy of the collider to a TeV or greater in an unobstrusive and adiabatic fashion with improvements that can be expected in the rf system of the main accelerators. The physical layout that we have chosen for the main linacs and their power sources (Fig. 3.19) provides access that allows upgrade of the rf system even as the collider is operating; for example, by taking one or a few stations off-line at a time. Our choice of X-band rf technology has been made to assure that accelerating gradients that approach 100 MV/m can ultimately be used without electrical breakdown or generation of unacceptable levels of dark current, and there are a number of possible advances in X-band technology that would lead to the TeV energy. We have based our design on what we believe to be improvements that are near-term and can reasonably be expected to occur in klystron and pulse compression technologies.

Tests with a prototype X-band klystron have already proven that output powers of 75 MW can be achieved, and a likely path to the TeV energy goal is taken by replacing and doubling the number of klystrons used in the main acelerator (dashed lines in Fig. 3.16).

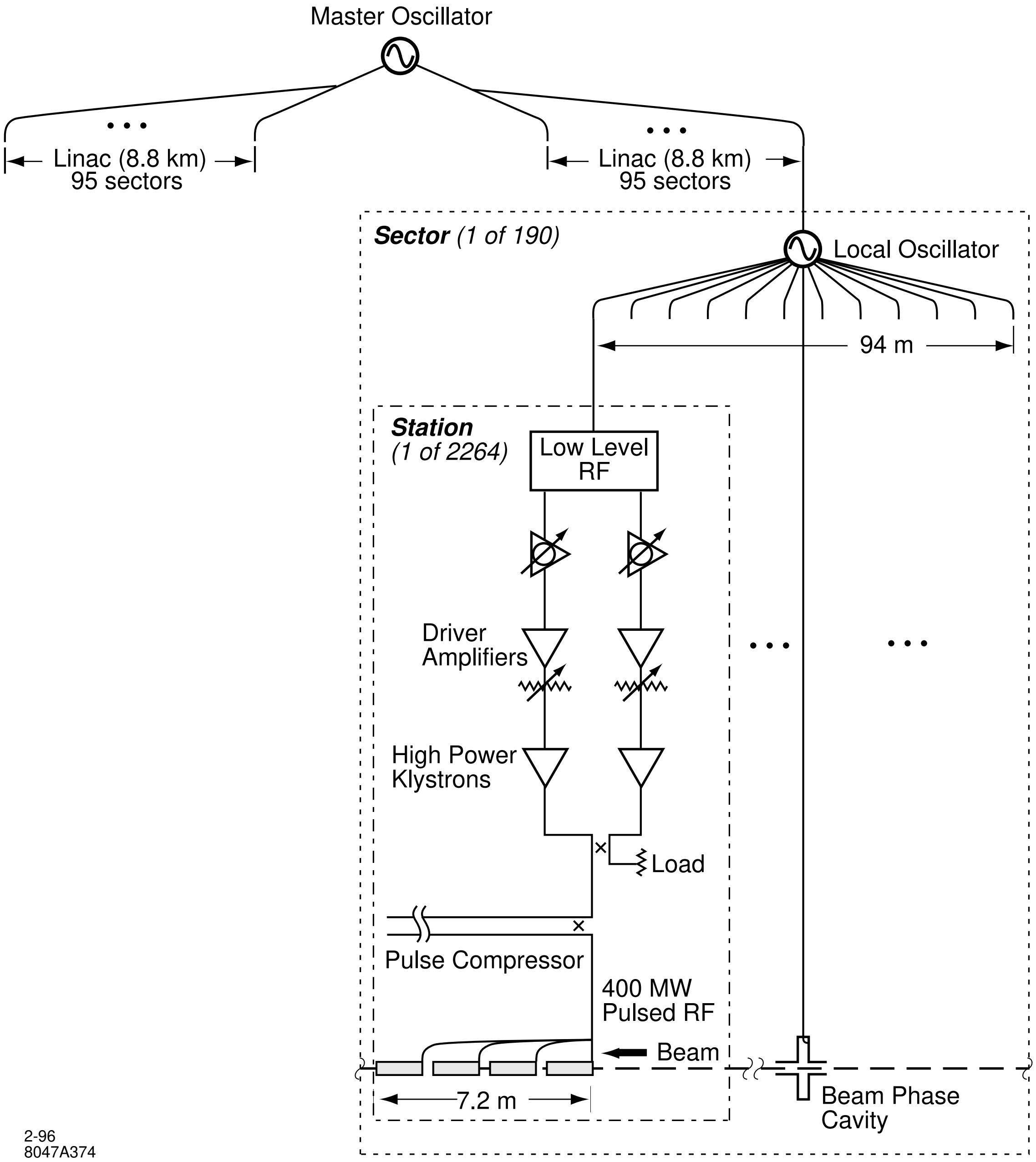

Figure 3.22: Schematic of rf drive system. The master oscillator provides phase-stable rf to local oscillators in each sector over a fiber distribution system. Local sources in each sector provide 11.424 GHz to each rf station in the sector using coaxial lines. A beam-phase cavity uses the beam to determine the rf phase for optimum operation. Power levels are low (several milliwatts) until the final drive for the high-power klystrons.

Although the klystron power rating necessary for the full 1 TeV has been achieved, the power conversion efficiency of the present tubes (approximately 48%) is not sufficiently high to maintain the total power consumed by the linac to an acceptable level (taken to be about 200 MW). Klystrons of the generation now being developed with PPM focusing are expected, according to computer modeling, to achieve conversion efficiencies of nearly 60%.

There are additional improvements that we anticipate will occur in X-band technologies that will lead to still higher overall power efficiencies. The finite filling time of the energy storage technique used in the SLED-II pulse compressor wastes power and results in an intrinsic 20% loss that could be avoided with the development of new microwave switching techniques. Initial experimental investigations of an optically triggered silicon switch show promise, and effort is continuing to develop a usable device based on this idea [18, 19]. First tests of an alternate compression scheme, binary pulse compression (BPC), have also been carried out, and have proven that this technique, though more expensive than SLED-II, works well with intrinsic efficiency of 100%. [20, 21]. A nice feature of the BPC scheme is that it reuses nearly all of the hardware of the SLED-II systems, so that if conversion to BPC were necessary, then a station-by-station modification is mechanically reasonable.

Final tests of any of these upgrade paths remain to be done. It will be important to verify the power ratings and efficiencies of not only the power generating components, but also those of the entire system. This will be one of the primary goals of the experimental program of the NLCTA.

To obtain the full 1 TeV energy and to maintain the linac power consumption below 200 MW, the klystron upgrade to 75 MW and elimination of the intrinsic power loss of the SLED-II system must be accomplished. From our experience to date, we believe it is reasonable to expect the net efficiency of the rf system to be increased from the initial design value of about 30% to the 40% required for the upgrade. The total length of the main linacs must also be increased slightly, from 16.3 to 17.7 km, but even if this additional length is not provided, the upgraded center-of-mass energy will still reach 925 GeV. This set of parameters is summarized in Table 3.10. Some of these potential improvements may, in fact, be ready in time to be included in the initial 500-GeV machine. This would result in additional performance margin or cost reductions. The 500-GeV parameters listed in Table 3.10 are conservatively based on experience with, and measurements on, prototypes which exist at the present time.

3.7.7 Outlook

The design of the rf system for the main linacs of the NLC is supported by existing and planned developmental prototypes, and by the NLCTA. Key NLC parameters such as the klystron power, acceleration gradient, and pulse-compression power gain have been exceeded in prototype systems. The next steps in the development program are completion of the NLCTA, the first damped and detuned structure, and the first PPM klystron prototype. The design of the NLC high-power rf system is mature and is now progressing toward detailed engineering considerations. Because of the magnitude of the project, special emphasis is being placed on designing for manufacturability and for overall system reliability.